

The boring history of Gaia BH3 from isolated binary evolution

Giuliano Iorio^{1,2,3*}, Stefano Torniamenti^{4,2**}, Michela Mapelli^{4,1,2,3***}, Marco Dall’Amico^{1,2}, Alessandro A. Trani⁵, Sara Rastello⁶, Cecilia Sgalletta^{2,7}, Stefano Rinaldi^{1,4}, Guglielmo Costa^{8,3}, Bera A. Dahl-Lahtinen¹, Gastón J. Escobar^{1,2}, Erika Korb^{1,2}, M. Paola Vaccaro⁴, Elena Lacchin^{1,2,4,9}, Benedetta Mestichelli^{4,10,11}, Ugo N. Di Carlo⁷, Mario Spera⁷, Manuel Arca Sedda^{10,11,12},

¹ Physics and Astronomy Department Galileo Galilei, University of Padova, Vicolo dell’Osservatorio 3, I-35122, Padova, Italy

² INFN - Padova, Via Marzolo 8, I-35131 Padova, Italy

³ INAF – Padova, Vicolo dell’Osservatorio 5, I-35122 Padova, I

⁴ Institut für Theoretische Astrophysik, ZAH, Universität Heidelberg, Albert-Ueberle-Straße 2, D-69120, Heidelberg, Germany

⁵ Niels Bohr International Academy, Niels Bohr Institute, Blegdamsvej 17, 2100 Copenhagen, Denmark

⁶ Departament de Física Quàntica i Astrofísica, Institut de Ciències del Cosmos, Universitat de Barcelona, Martí i Franquès 1, E-08028 Barcelona, Spain

⁷ SISSA, via Bonomea 365, I-34136 Trieste, Italy

⁸ Univ Lyon, Univ Lyon1, ENS de Lyon, CNRS, Centre de Recherche Astrophysique de Lyon UMR5574, F-69230 Saint-Genis-Laval, France

⁹ INAF, Osservatorio Astronomico di Bologna, Via Gobetti 93/3, I-40129 Bologna, Italy

¹⁰ Gran Sasso Science Institute, Via F. Crispi 7, I-67100 L’Aquila, Italy

¹¹ INFN - Laboratori Nazionali del Gran Sasso, I-67100 L’Aquila, Italy

¹² INAF - Osservatorio Astronomico d’Abruzzo, Via Mentore Maggini, s.n.c., I-64100 Teramo, Italy

Received September 15, 1996; accepted March 16, 1997

ABSTRACT

Gaia BH3 is the first observed dormant black hole (BH) with a mass of $\approx 30 M_{\odot}$ and represents the first confirmation that such massive BHs are associated with metal-poor stars. Here, we explore the isolated binary formation channel for Gaia BH3 focusing on the old and metal-poor stellar population of the Milky Way halo. We use the `mist` stellar models and our open-source population synthesis code `SEVN` to evolve 3.2×10^8 binaries exploring 16 sets of parameters, that encompass different natal kicks, metallicities, common-envelope efficiencies, and models for the Roche-lobe overflow. We find that systems like Gaia BH3 form preferentially from binaries initially composed of a massive star ($40 - 60 M_{\odot}$) and a low mass companion ($< 1 M_{\odot}$) in a wide ($P > 10^3$ days) and eccentric orbit ($e > 0.6$). Such progenitor binary stars do not undergo any Roche-lobe overflow episode during their entire evolution, so that the final orbital properties of the BH-star system are essentially determined at the core collapse of the primary star. Low natal kicks (≈ 10 km/s) significantly favour the formation of Gaia BH3-like systems, but high velocity kicks up to ≈ 220 km/s are also allowed. We estimate the formation efficiency for Gaia BH3-like systems in old ($t > 10$ Gyr) and metal-poor ($Z < 0.01$) populations to be $4 \times 10^{-8} M_{\odot}^{-1}$ (for our fiducial model), representing $\approx 3\%$ of the whole simulated BH-star population. We expect up to ~ 3000 BH-star systems in the Galactic halo formed through isolated evolution, of which ~ 100 are compatible with Gaia BH3. Gaia BH3-like systems represent a common product of isolated binary evolution at low metallicity ($Z < 0.01$), but given the steep density profile of the Galactic halo we do not expect more than one at the observed distance of Gaia BH3. Considering the estimated formation efficiency for both the isolated and dynamical formation channel, we conclude that they are almost equally likely to explain the origin of Gaia BH3.

Key words. black hole physics – methods: numerical – binaries: general – stars: black holes – stars: massive – Galaxy: halo

1. Introduction

Gaia data (Gaia Collaboration et al. 2023) offer a unique opportunity to search for dormant black holes (BHs), i.e. X-ray and radio-quiet BHs that are members of a binary system with a star (Guseinov & Zel’dovich 1966; Trimble & Thorne 1969). Gaia BH3, the third dormant BH retrieved from these data, has a mass of $\sim 33 M_{\odot}$ and is member of a loose eccentric binary system (orbital period $P \approx 4000$ days, eccentricity $e \approx 0.72$) together with a $\approx 0.76 M_{\odot}$ very metal-poor giant star ($[\text{Fe}/\text{H}] = -2.56 \pm 0.12$ from the UVES spectrum, Gaia Collaboration et al. 2024).

Gaia BH3 is the first ever discovered dormant BH with mass $\geq 30 M_{\odot}$, and the first BH with such a high mass unequivocally observed in the Milky Way. The other two Gaia BHs (BH1 and

BH2) both have a mass of $\sim 10 M_{\odot}$ (El-Badry et al. 2023b,a; Tanikawa et al. 2024). All of the other dormant BH candidates (Casares et al. 2014; Ribó et al. 2017; Giesers et al. 2018, 2019; Thompson et al. 2019; Shenar et al. 2022a,b; Mahy et al. 2022; Lennon et al. 2022; Saracino et al. 2022, 2023) and the BHs in X-ray binary systems with a dynamical measurement have mass between a few and $\approx 20 M_{\odot}$ (Oëzel et al. 2010; Miller-Jones et al. 2021).

BHs with mass $\geq 30 M_{\odot}$ have been observed for the first time with gravitational waves (Abbott et al. 2016a,b, 2021a,c,b). According to the main formation scenario, such massive BHs are expected to form from metal-poor stars, which do not lose much mass by stellar winds and collapse to a BH directly (Heger & Woosley 2002; Mapelli et al. 2009, 2010, 2013; Zampieri & Roberts 2009; Belczynski et al. 2010; Fryer et al. 2012; Ziosi et al. 2014; Spera et al. 2015). Gravitational-wave data have proved the existence of such "oversize" BHs, but they do not carry any information about the progenitor’s metallicity, because

* giuliano.iorio.astro@gmail.com

** stefano.torniamenti@uni-heidelberg.de

*** mapelli@uni-heidelberg.de

we did not observe any electromagnetic counterpart. Hence, Gaia BH3 is the first direct confirmation that BHs with mass in excess of $30 M_{\odot}$ are associated with metal-poor stellar populations, supporting the main theoretical scenario.

For both its chemical composition and Galactic orbit, Gaia BH3 is associated with the ED–2 stream, composed of stars that are at least 12 Gyr old (Balbinot et al. 2024). Thus, this is the first BH unambiguously associated with a disrupted star cluster with a mass $2 \times 10^3 - 4.2 \times 10^4 M_{\odot}$ (Balbinot et al. 2024). Preliminary numerical models show that Gaia BH3 might have assembled dynamically from a low-mass star and a BH that have not evolved in the same binary star system (Marín Pina et al. 2024, Arca Sedda et al. 2024, in prep.).

While the association of Gaia BH3 with the ED–2 stream is indisputable, here we show that this system is compatible with the nearly unperturbed evolution of a primordial binary star: our population-synthesis simulations show that we do not need to invoke a dynamical exchange or a dynamical capture to explain its orbital properties (see also El-Badry 2024).

Gaia BH3 is very different from both Gaia BH1 and Gaia BH2, which challenge our models of binary evolution (El-Badry et al. 2023b,a; Tanikawa et al. 2023; Rastello et al. 2023; Di Carlo et al. 2024; Generozov & Perets 2024; Kotko et al. 2024): its wide orbital separation does not require evolution via Roche-lobe overflow or common envelope. Rather, it is consistent with a wide system that never went through mass transfer and survived the formation of the BH because this happened via direct collapse, with a mild natal kick. We show that the measured orbital eccentricity helps to constrain the phase of the binary at the time of the formation of the BH. If formed in a star cluster, Gaia BH3 might have evolved nearly unperturbed inside it, until it evaporated or was ejected. The paper is organized as follows. We describe our methodology in Section 2, present the main results in Section 3, and discuss the implications in Section 4. Section 5 summarizes our main takeaways.

2. Methods

In this work, we compare the observational features of the Gaia BH3 system with a synthetic population of stellar binaries produced with the Stellar EVolution for N-body (SEVN) code (Spera & Mapelli 2017; Spera et al. 2019; Mapelli et al. 2020; Iorio et al. 2023). In SEVN, the evolution of single stars is estimated by interpolating on the fly across pre-calculated stellar evolution tracks stored in custom lookup tables. The models presented in this study are computed using the MIST stellar tracks by Choi et al. (2016). We used TRACKCRUNCHER (Iorio et al. 2023) to produce the SEVN tables from the MIST stellar tracks. We produce eight sets of tables from metallicity $Z = 1.4 \times 10^{-5}$ to 4.5×10^{-2} ; each set contains stellar tracks from $0.71 M_{\odot}$ to $150 M_{\odot}$.

In SEVN, binary interactions are described through analytical and semi-analytical prescriptions, encompassing stable mass transfer by Roche-lobe overflow and winds, common envelope evolution, angular momentum dissipation by magnetic braking, tidal interactions, orbital decay by gravitational-wave emission, dynamical hardening, chemically homogeneous evolution, and stellar mergers. In our models, we treat tidal forces with the analytical formalism developed by Hut (1981), as implemented by Hurley et al. (2002). For more details, we refer to Iorio et al. (2023).

In this work, we use the SEVN version V 2.8.0 (commit 3375978) publicly available at the GitLab repository <https://gitlab.com/sevncodes/sevn>. The code TRACKCRUNCHER used

to produce the MIST table is available at <https://gitlab.com/sevncodes/trackcruncher> (commit 0827337).

2.1. Initial conditions

We have generated the initial conditions for 2×10^7 binary systems by extracting the zero-age main-sequence mass of the primary (more massive) star, m_1 , from the Kroupa initial mass function (Kroupa 2001) from 5 to $150 M_{\odot}$. The mass of the secondary (less massive) star is set from the binary mass ratio q following the distribution $\text{PDF}(q) \propto q^{-0.1}$ with $q \in [0.71 M_{\odot}/m_1, 1]$. We have drawn the initial orbital period (P) and eccentricity (e) from the following distributions: $\text{PDF}(\log P/\text{days}) \propto (\log P)^{-0.55}$, $\text{PDF}(e) \propto e^{-0.42}$. These distributions of mass ratios, orbital periods and eccentricities are fitting formulas to observations of massive binary stars in Galactic young clusters (Sana et al. 2012). The periods range from 1.4 days to 866 years, while the eccentricities range from 0 to $e_{\text{max}} = 1 - (P/2 \text{ days})^{-2/3}$, according to Moe & Di Stefano (2017). The total mass of the simulated population is $M_{\text{sim}} = 4.2 \times 10^8 M_{\odot}$ corresponding to a mass of $M_{\text{tot}} = 1.4 \times 10^9 M_{\odot}$ when accounting for the fact that we do not simulate low-mass primary stars and systems with secondary stars less massive than $0.71 M_{\odot}$ ¹. We use SEVN to evolve all the generated binaries from the zero age main sequence up to the moment in which the two stars are compact remnants (white dwarfs, neutron stars, BHs).

2.2. Fiducial model

In our fiducial model, we use the default SEVN options as described by Iorio et al. (2023) (see also Sgalletta et al. 2023; Costa et al. 2023) except for the circularisation option. Here, we use the new default circularisation option *angmom* in which at the onset of the Roche-lobe overflow the orbit is circularised conserving the angular momentum, so the new semi-major axis is $a_{\text{new}} = a_{\text{old}}(1 - e_{\text{old}}^2)$.

The stability of the Roche-lobe mass transfer is checked by comparing the current binary mass ratio to a critical mass ratio that depends on the stellar evolutionary phase. In this work, we use the default option of SEVN (Iorio et al. 2023), in which Roche-lobe overflow episodes involving stars with radiative envelope (main sequence stars and low-mass stars before climbing the red giant branch) are always stable, while in all the other cases we use the value of the critical mass ratio by Hurley et al. (2002). When the mass transfer is unstable, a common envelope evolution phase begins (Ivanova et al. 2013). We use the standard α – λ prescription for the common envelope (Webbink 1984; Hurley et al. 2002, and reference therein) with the ejection efficiency parameter $\alpha = 1$, whereas we estimate λ using the formalism by Claeys et al. (2014), as implemented in SEVN (see Appendix A1.4 in Iorio et al. 2023).

After a core-collapse supernova, we decide the mass of the BH based on the delayed model by Fryer et al. (2012). We adopt the supernova kick model by Giacobbo & Mapelli (2020), where the natal kick is drawn from a Maxwellian distribution with one-dimensional root-mean-square $\sigma_{\text{rms}} = 265 \text{ km/s}$ (Hobbs et al. 2005), re-scaled by the ejecta mass and the compact-remnant mass resulting in a much lower ($\lesssim 10 \text{ km/s}$) effective kick for the massive BHs ($> 30 M_{\odot}$).

In the fiducial model, we set the metallicity to $Z = 4.1 \times 10^{-5}$, corresponding to the observed value of $[\text{Fe}/\text{H}] = -2.56$

¹ We assume a parent population with primary masses m_1 between $0.08 M_{\odot}$ and $150 M_{\odot}$, and mass-ratios in the range $q \in [0.08 M_{\odot}/m_1, 1]$.

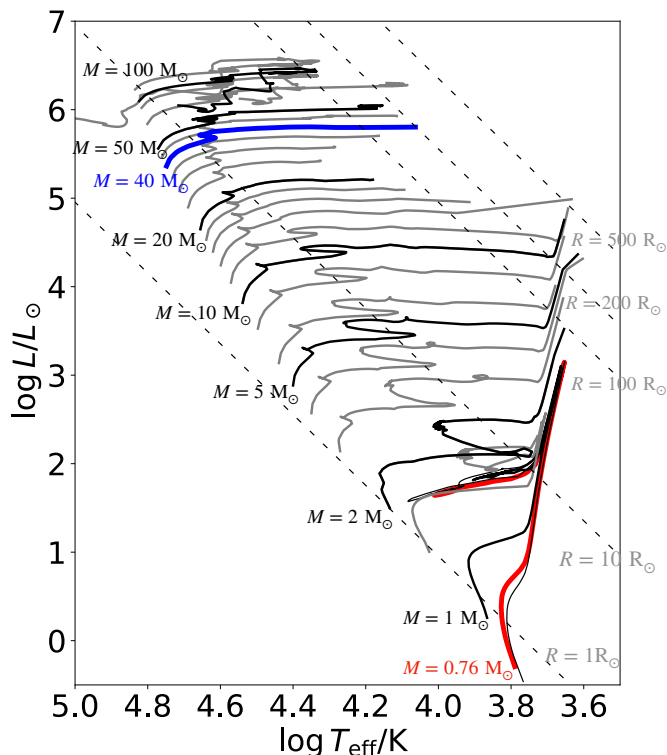


Fig. 1: Hertzsprung–Russell diagram of a sample of stars at metallicity $Z = 4.1 \times 10^{-5}$ interpolated by *SEVN* from the *MIST* stellar tracks. The blue and red lines show the likely progenitors of the BH and stellar companion in Gaia BH3, respectively.

considering the *MIST* stellar models. The *MIST* stellar tracks with the fiducial metallicity are shown in Figure 1.

2.3. Additional models: parameter-space exploration

To explore the parameter space for the formation of Gaia BH3-like systems, we ran an additional set of 15 simulations varying one parameter of the fiducial simulation per time. For the initial conditions, we used the same set of 2×10^7 binary systems as for the fiducial model.

We have simulated eight additional metallicities: $Z = 0.0001$ (model Z1E-4), $Z = 0.0004$ (model Z4E-4), $Z = 0.0008$ (model Z8E-4), $Z = 0.001$ (model Z1E-3), $Z = 0.004$ (model Z4E-3), $Z = 0.006$ (model Z6E-3), $Z = 0.008$ (model Z8E-3), and $Z = 0.01$ (model Z1E-2). We have also explored the effect of the supernova kick by running four different simulations in which the kicks are drawn from a Maxwellian distribution with $\sigma_{\text{rms}} = 1$ km/s (essentially no kick, model VK1), 50 km/s (VK50), 100 km/s (VK100), and 265 km/s (VK265). In these models, the kick is not re-scaled for the ejected mass and the mass of the compact remnant. We also test the importance of the common-envelope phase by running two simulations varying the common-envelope efficiency: $\alpha = 3$ (model CE α 3) and $\alpha = 5$ (model CE α 5). Higher common-envelope efficiency enhances the likelihood of system survival without merger, leading to increased post-common envelope orbital separation.

Finally, we have run an additional model (RLOp) in which we allow the system to start a Roche-lobe overflow in an eccentric orbit if the condition of Roche-lobe overflow is satisfied at the periastron, i.e. if the stellar radius is larger than

$R_L = r_{\text{peri}} f(q)$, where r_{peri} is the periastron and $f(q)$ is a function that depends on the binary mass ratio (Eggleton 1983).

3. Results

Figure 2 shows the properties of the BH-star systems in the fiducial model. We consider all the simulation outputs in which a binary system is composed of a BH and a giant star, i.e. a star that left the main sequence and has not started the core helium burning phase yet. We impose the additional condition that the system is not undergoing a common-envelope or Roche-lobe overflow episode. The color map of Fig. 2 represents the time spent by all the systems in such configuration, which is a proxy of the likelihood to observe a given system.

Binaries hosting a BH and a massive companion are, in general, more common in the simulations, but the short lifetime of the massive star makes them less likely to be observed. In contrast, BH-low mass star binaries are rarer, but once formed, they can remain in the same configuration for several Gyrs.

Gaia BH3 is located in a region of the parameter space well covered by the fiducial simulation, especially if we consider binary systems older than 10 Gyr. In addition, the Gaia BH3 properties (mostly period and BH mass) cover a range in which Gaia is particularly sensible to astrometric signals of binarity (see e.g. Penoyre et al. 2022). From Figure 2, we can conclude that if a BH-star system is observed in an old and metal-poor population, it is not surprising to find it with the Gaia BH3 configuration. In this sense, Gaia BH3 is not an outlier, unlike Gaia BH1 and BH2 (El-Badry et al. 2023b; Rastello et al. 2023).

It is convenient to define a region of the observed parameter space to identify Gaia BH3-like systems. For the sake of simplicity, and to help the comparison with previous work, we use the same selection cut used in Marín Pina et al. (2024): $P \in [400, 40000]$ days, $m_s \in [0.2, 1] M_\odot$, $m_{\text{bh}} \in [25, 45] M_\odot$, $e \in [0.63, 0.83]$. The box represents about 1% of the volume of the parameter space that includes BH-star systems at ages older than 10 Gyr.

3.1. Formation history

All the Gaia BH3-like systems in our models have the same simple formation history. Their progenitors consist of a massive star ($> 40 M_\odot$) and a low mass companion ($< 1 M_\odot$). The binary components never interact through Roche-lobe overflow, so the orbital properties at BH formation are almost the same as their initial ones. The final properties of the BH-star system are then determined by the binary phase at the moment of the supernova explosion, the amount of mass lost during the evolution, and the BH natal kick.

In our fiducial model, the initial BH progenitor mass is about $40\text{--}50 M_\odot$ and the ejected mass at BH formation is $10\text{--}20 M_\odot$. The mild BH natal kick (~ 10 km/s) cannot drastically change the binary orbital parameters. As a consequence, the large majority of BH progenitors originated with very similar orbital properties to Gaia BH3: a period between 10^3 and 10^4 days and an eccentricity in the range $0.6\text{--}0.9$. The system more similar to Gaia BH3 has an initial period of about 1500 days, an eccentricity of 0.65, stellar mass of $0.83 M_\odot$ and initial BH progenitor mass of $41 M_\odot$. We find a sub-population ($< 10\%$ of the total) that produces Gaia BH3-like systems starting from almost circular orbits ($e < 0.2$) and lower initial periods ($< 10^3$ days). For these systems, the final orbital properties are determined by the high value of the BH natal kick. A few systems ($\approx 3\%$) have

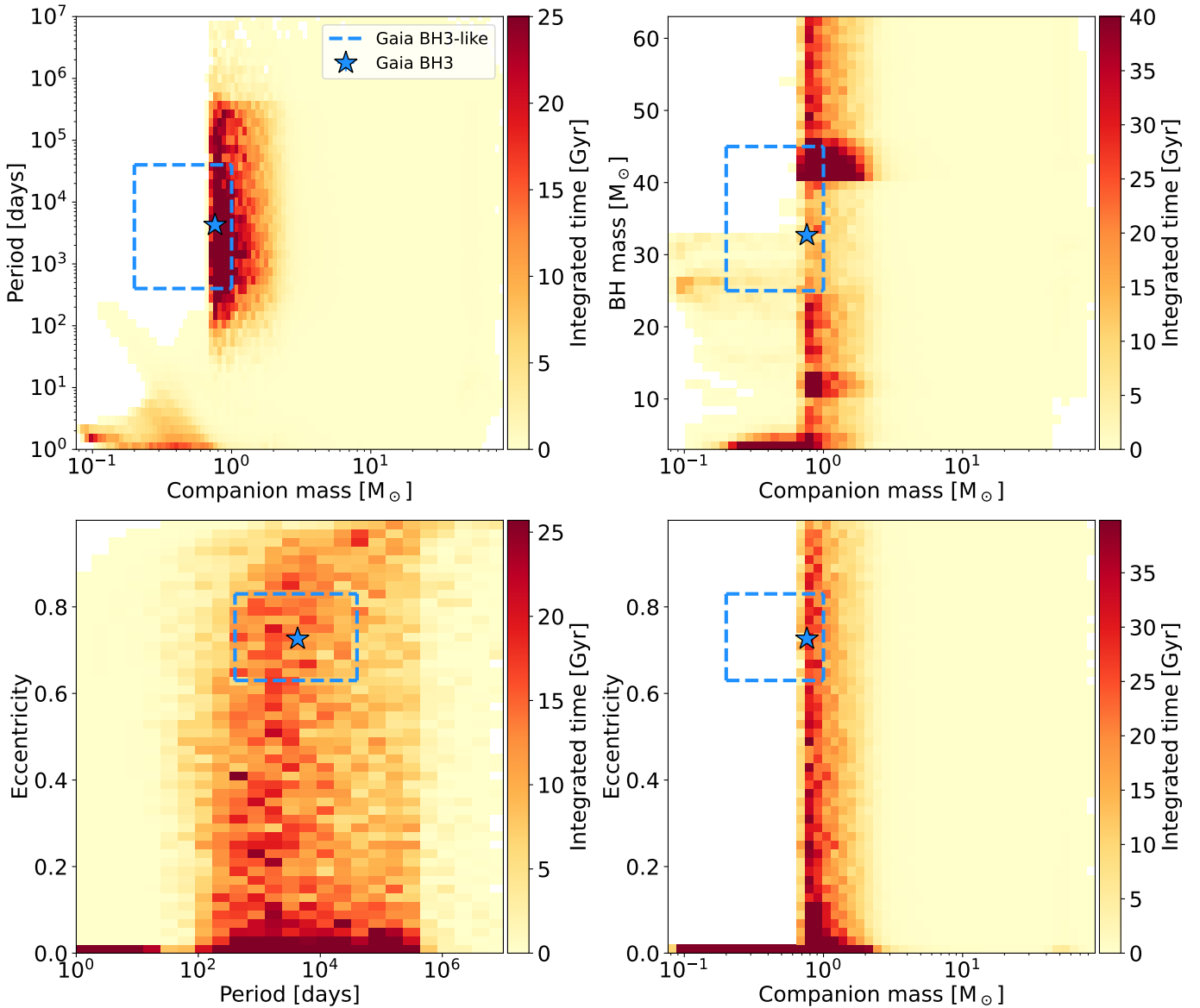


Fig. 2: Properties of non-interacting BH-star systems in the fiducial model. Here, we only show stars in the giant phase, i.e. outside the main sequence and that have not started the core helium burning phase yet. Also, we do not show systems that undergo a Roche-lobe overflow episode. From top to bottom and from left to right: orbital period versus companion star mass; BH mass versus companion star mass; eccentricity versus orbital period; eccentricity versus companion star mass. The color map shows the integrated time spent by the systems in a given bin, thus it is a proxy of the likelihood to observe a system with such properties. The map does not include information about the stellar luminosity, which is also important for detectability. We assume a metallicity $Z = 4.1 \times 10^{-5}$. The star indicates the properties of Gaia BH3, while the light blue boxes show the criteria used to select Gaia BH3-like systems (hereafter, Gaia BH3box). The color maps saturate at 98% of the maximum value.

very massive BH progenitors of about $120 M_{\odot}$, which produce BHs with a mass of $\sim 30 M_{\odot}$ because of mass loss during pulsational pair instability (Heger & Woosley 2002; Belczynski et al. 2016; Woosley 2017, 2019; Farmer et al. 2019; Costa et al. 2021; Tanikawa et al. 2021).

Since Gaia BH3-like progenitors do not experience any binary interaction, there are no differences for the model CE α 3 and CE α 5. Also, we obtain the same results for the model RLOp, which indicates that including or not the possibility to trigger a stable mass transfer at the periastron is not important for the production of such binary systems. We find the same progenitors in the case of the kick model VK1, as a confirmation that in the

fiducial model the implemented kick model produces very low kicks for the case of Gaia BH3-like progenitors.

Models with higher kick velocities show significant differences in the initial orbital properties. The BH natal kicks in models VK50 and VK100 are able to wash out any correlation between the initial and final period and eccentricity. The Gaia BH3-like progenitors have initial periods and eccentricities almost uniformly distributed in the range 100–4000 days, and 0–0.8, respectively. At very high velocities (model VK265) the formation of Gaia BH3-like binaries is strongly suppressed. Most systems break during BH formation and just a few of them (4 over 20 million simulated binaries) had a lucky configuration of

binary phase and/or velocity kick that let them survive the supernova event.

We find a trend with metallicity for the initial orbital period, eccentricity and BH progenitor mass. From low metallicity (model Z1E-4) to intermediate-high metallicity (model Z1E-2) the lower limit of the initial period moves toward higher values ($P > 1000$ days for model Z1E-2), while the sub-populations with initial low eccentricity ($e < 0.6$) tend to disappear. As for the BH progenitor mass, the range of values widens with increasing metallicity, up to initial masses of $100 M_{\odot}$. This is due to the non-monotonic trend of the initial BH mass relation of the `MIST` tracks used in this work when paired with the rapid and delayed supernova models by Fryer et al. (2012). When assuming initial masses lower than $60 M_{\odot}$, the combination of the Fryer et al. (2012) supernova models and the `MIST` tracks produces BHs more massive than 25 and $30 M_{\odot}$ up to a metallicity $Z = 0.02$ and 0.01 , respectively. Relaxing the limit on the initial masses, BHs more massive than $30 M_{\odot}$ are excluded only for $Z > 0.02$.

3.2. Bayesian sampling

The `SEVN` simulations indicate that the region of Gaia BH3 in the observed parameter space (P , e , m_{BH} , m_{ms}) tends to be populated by systems in which the binary components never interact. Therefore, the final binary properties are determined by the initial binary parameters and the details of the BH formation only. In order to focus on Gaia BH3 progenitors independently of the chosen selection cut, we implement a simple Bayesian sampling technique in which we sample the posteriors of the binary initial condition using as likelihood a multivariate normal distribution centred on the Gaia BH3 value and with standard deviation equal to the reported errors (assumed independent).

For the parameter prior we use a uniform distribution for the mean anomaly (between 0 and 2π) at the moment of the BH formation, a uniform distribution for the mass of the BH progenitor (between 20 and $100 M_{\odot}$) and eccentricity (between 0 and 1), a log-uniform distribution for the period (between 10 and 10^6 days), and a normal distribution for the three spherical components of the velocity kick, corresponding to a Maxwellian distribution of the velocity module.

We test five different values of the one-dimensional root-mean-square velocity for the Maxwellian distribution ($1, 10, 50, 100, 256$ km/s). We also exclude interacting binary systems, by setting the prior to be equal to 0 when the maximum radius of the BH progenitor is larger than either the separation at periastron or the Roche-lobe radius at periastron (see Section 2). To estimate the final properties of the binary we use the formalism in Appendix of Hurley et al. (2002) and we estimate the maximum radius and the final mass of the BH progenitor by using `SEVN`. The posteriors are sampled using the Monte-Carlo Markov Chain (MCMC) Ensemble Sampler available in the `emcee` python package (Foreman-Mackey et al. 2013). This method is similar to the grid search presented by El-Badry (2024), but our method is tailored to reproduce exactly the observed properties of Gaia BH3, exploring widely the parameter space. In particular, we do not assume initial circular orbits and this has a significant impact on the final results. Since we include the reduction of the parameter space due to stellar interactions directly in the priors, the posteriors do not need to be corrected a posteriori.

We show the posterior samples in Figure 3. Overall, they are consistent with what obtained from the `SEVN` simulations of the wider space of the selection cut assumed in Sect. 3.1. Assuming low kick velocities, the Gaia BH3 progenitor is very likely

Model	$\eta_{\text{GaiaBH3-like}}$	$\eta_{\text{GaiaBH3-like}} (t > 10 \text{ Gyr})$	$\eta_{\text{BHStar}} (t > 10 \text{ Gyr})$
fiducial	$(1.1 \pm 0.1) \times 10^{-7}$	$(4.7 \pm 0.6) \times 10^{-8}$	$(1.5 \pm 0.1) \times 10^{-6}$
RLOp	$(1.1 \pm 0.1) \times 10^{-7}$	$(4.0 \pm 0.5) \times 10^{-8}$	$(1.5 \pm 0.1) \times 10^{-6}$
VK1	$(1.1 \pm 0.1) \times 10^{-7}$	$(4.3 \pm 0.6) \times 10^{-8}$	$(2.2 \pm 0.1) \times 10^{-6}$
VK50	$(9.0 \pm 0.8) \times 10^{-8}$	$(3.9 \pm 0.5) \times 10^{-8}$	$(5.0 \pm 0.2) \times 10^{-7}$
VK100	$(4.0 \pm 0.5) \times 10^{-8}$	$(1.3 \pm 0.3) \times 10^{-8}$	$(5.0 \pm 0.2) \times 10^{-7}$
VK265	$(6.4 \pm 2.1) \times 10^{-9}$	$(2.1 \pm 1.2) \times 10^{-9}$	$(5.4 \pm 0.2) \times 10^{-8}$
CE α 3	$(1.1 \pm 0.1) \times 10^{-7}$	$(4.7 \pm 0.6) \times 10^{-8}$	$(2.1 \pm 0.1) \times 10^{-6}$
CE α 5	$(1.1 \pm 0.1) \times 10^{-7}$	$(4.7 \pm 0.6) \times 10^{-8}$	$(2.4 \pm 0.1) \times 10^{-6}$
Z1E-4	$(1.3 \pm 0.1) \times 10^{-7}$	$(4.8 \pm 0.6) \times 10^{-8}$	$(1.4 \pm 0.1) \times 10^{-6}$
Z4E-4	$(1.1 \pm 0.1) \times 10^{-7}$	$(4.8 \pm 0.6) \times 10^{-8}$	$(1.4 \pm 0.1) \times 10^{-6}$
Z8E-4	$(9.4 \pm 0.8) \times 10^{-8}$	$(3.9 \pm 0.5) \times 10^{-8}$	$(1.5 \pm 0.1) \times 10^{-6}$
Z1E-3	$(9.2 \pm 0.8) \times 10^{-8}$	$(4.0 \pm 0.5) \times 10^{-8}$	$(1.6 \pm 0.1) \times 10^{-6}$
Z4E-3	$(9.1 \pm 0.8) \times 10^{-8}$	$(5.3 \pm 0.6) \times 10^{-8}$	$(2.4 \pm 0.1) \times 10^{-6}$
Z6E-3	$(9.4 \pm 0.8) \times 10^{-8}$	$(5.8 \pm 0.6) \times 10^{-8}$	$(2.7 \pm 0.1) \times 10^{-6}$
Z8E-3	$(8.2 \pm 0.8) \times 10^{-8}$	$(6.2 \pm 0.7) \times 10^{-8}$	$(3.1 \pm 0.1) \times 10^{-6}$
Z1E-2	$(8.2 \pm 0.8) \times 10^{-8}$	$(7.1 \pm 0.7) \times 10^{-8}$	$(3.4 \pm 0.1) \times 10^{-6}$

Table 1: Formation efficiency (M_{\odot}^{-1}) obtained from different `SEVN` simulations. The column reports the formation efficiency for the the Gaia BH3 selection cut (see text), the same selection cut but only for systems that are still in the BH-star configuration after 10 Gyr, and for all the BH-star systems with age larger than 10 Gyr. The formation efficiency assumes a 100% binary fraction. The errors are estimated as the square root of the counts over the total mass.

to originate from a wide and eccentric binary ($P \approx 3500$ days, $e \sim 0.75$). The smaller peak at around 10^3 days and $e \sim 0.4$ is due to systems that form the BH at periastron, where it is more favourable to produce large final eccentricities due to the impact of mass loss during the supernova explosion. Larger kicks widen the range of initial periods and eccentricities, with most of the initial periods around 500 – 600 days. The period distribution is sharply cut below 300 days because the objects are tight enough to interact. It is possible to form a Gaia BH3 system with initial kicks up to 200 km/s. For higher values, the kick is larger than the escape velocity at periastron in the whole range of periods consistent with a non-interacting binary.

Independently of the explored parameters, a clear picture emerges. In presence of low supernova kicks (< 10 km/s), Gaia BH3 like systems form from non interacting binary progenitors preferentially in a wide ($500 < P/\text{days} < 2 \times 10^4$) and eccentric configuration. Alternatively, on the off-chance that the binary survives to higher supernova kicks, systems with Gaia BH3 properties can form preferentially from tighter ($P/\text{days} \sim 500$) systems almost independently of their initial eccentricity if $e < 0.7$. For this reason, the initial properties of the binary can play a key role in setting the formation efficiency of Gaia BH3-like systems.

3.3. Halo population

In the explored models, Gaia BH3-like systems represent one of the standard outcomes of binary evolution. We now investigate how common Gaia BH3-like systems and BH-star binaries are in the Galactic halo environment, characterised by low metallicity and old ages. We also assume $t > 10$ Gyr. First, we estimate the formation efficiency, defined as the ratio of the number of objects to the total simulated mass. We correct the total mass in the initial conditions for the incomplete mass sampling of the primary, and assume an initial binary fraction of 1 for the sake of simplicity. Table 1 reports the formation efficiency for all the

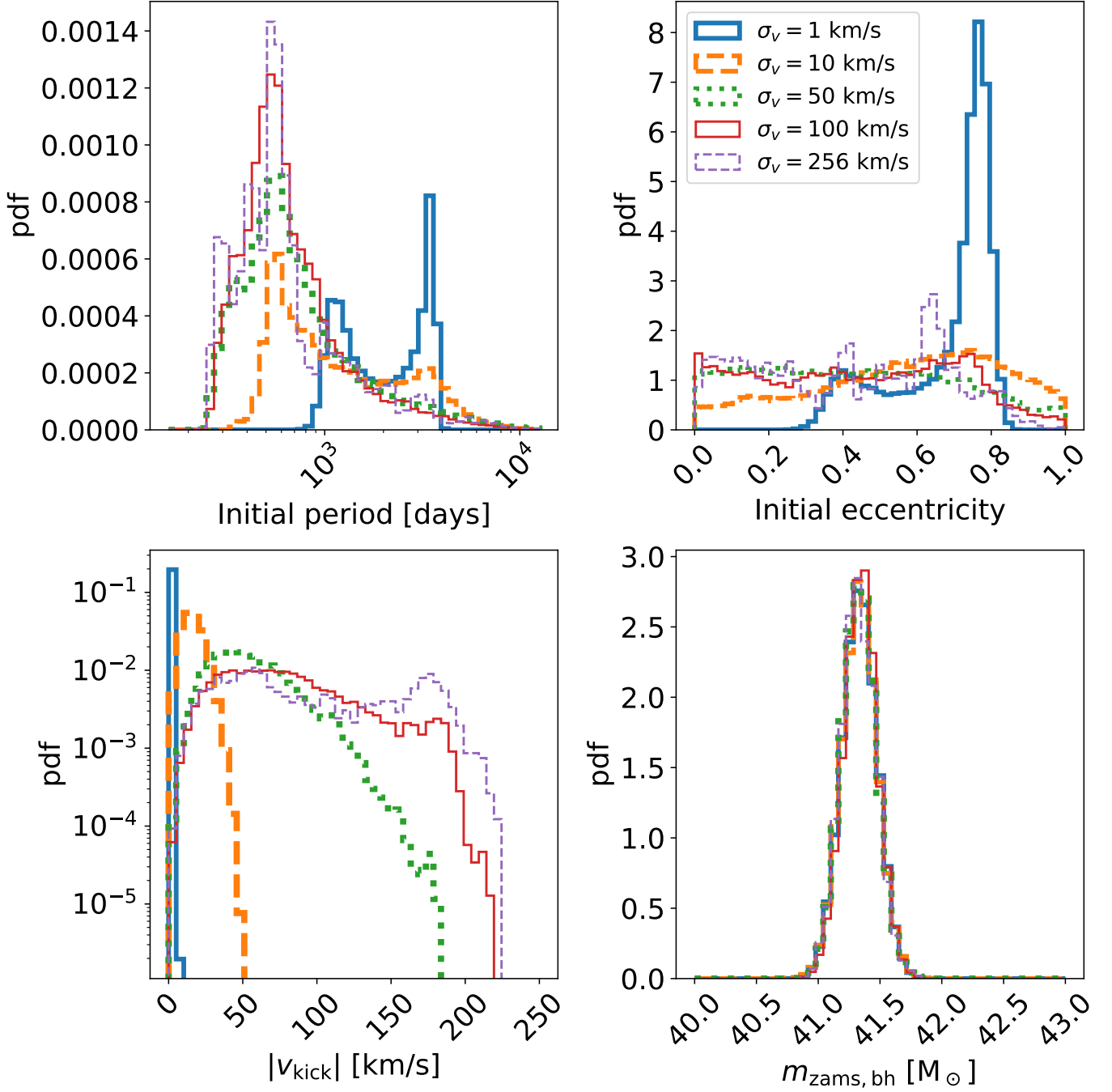


Fig. 3: Distribution of the initial conditions of the binaries that reproduce the Gaia BH3 properties after the BH formation. From top left to bottom right, the panels show the initial binary period, initial eccentricity, the module of the BH natal kick velocity, and initial mass of the BH progenitor. We show the distributions obtained assuming different Maxwellian-distribution priors for the kick velocity: $\sigma_v = 1$ km/s (blue, thick solid), $\sigma_v = 10$ km/s (orange, thick dashed), $\sigma_v = 50$ km/s (green, dotted), $\sigma_v = 100$ km/s (red, thin solid), $\sigma_v = 256$ km/s (violet, thin dashed).

systems in the Gaia BH3 selection box (Figure 2), and for those that are in the selection box and in the BH-star configuration after 10 Gyr.

In the fiducial model, the population of Gaia BH3-like objects accounts for about 3% of the whole population at $t > 10$ Gyr. This number is consistent with the volume fraction sampled by the selection box. Models with higher kicks significantly suppress the formation of both Gaia BH3-like and BH-star systems, while a higher metallicity increases their formation efficiency up

to a factor of two. Given the formation history of Gaia BH3-like objects, the efficiency is not affected by the choice of the common-envelope ejection efficiency. However, larger values of the common-envelope efficiency parameter α slightly increase the formation efficiency of the whole BH-star systems resulting in a lower fraction of Gaia BH3-like systems.

Even if the Galactic stellar halo is the least massive component of our Galaxy, the most recent estimates revise its mass from few $10^8 M_\odot$ (see e.g. Bell et al. 2008) up to $0.7 - 1.2 \times 10^9$

M_{\odot} (Deason et al. 2019; Lane et al. 2023). Combining the total halo mass with the formation efficiencies in Table 1, we predict a number of BH-stars in the halo in the range $\approx 1800 - 3000$. Among these systems, about 50 – 100 fall in the Gaia BH3 selection cut used in this work (Figure 2). The Galactic stellar halo is a diffuse component extended up to 100 kpc with a steep density profile ($\rho \propto r^{-\gamma}$, with $2 < \gamma < 5$, see e.g. Medina et al. 2024; Iorio et al. 2018, and references therein).

Deason et al. (2019) report a local density profile at Sun location of $\rho_{h,\odot} \approx 8 \times 10^4 M_{\odot}/\text{kpc}^3$. Multiplying this density by the formation efficiencies of the old BH-star binaries we obtain a local density of $n_{\text{BHStar}} = \eta_{\text{BHStar}} \rho_{h,\odot}$ ranging from 0.1 kpc^{-3} to 0.3 kpc^{-3} . The values correspond to an expected number of objects between 0.12 and 0.27 at the distance of Gaia BH3 ($\approx 0.6 \text{ kpc}$). At face value, we do not expect any BH-star binary system from the halo in the solar neighbourhood. However, we can account for the statistical noise assuming that the number of systems follows a Poissonian distribution with rate λ_{BHStar} ranging between 0.12 and 0.27. In this case, the probability to observe at least one object is between 11% and 25%. By simply using the formation efficiency for the old systems in the Gaia BH3 selection box (Figure 2) we obtain a Poisson rate between 0.003 and 0.006, corresponding to the probability to observe at least one Gaia BH3-like system of 0.3–0.6%. Although these numbers correspond to the very low probability tail of the distribution, they cannot be rejected at 3σ level. However, a single future detection of another of Gaia BH3-like binary system in the Galactic halo within the solar neighbourhood will be enough to significantly rule-out the isolated formation channel, according to the models presented in this work. However, this will represent a challenge also for the alternative dynamical formation channel (see Section 4.3).

4. Discussion

4.1. Initial eccentricity and stellar tides

In all the simulations assuming our fiducial kick model (Giacobbo & Mapelli 2020), Gaia BH3-like systems form preferentially from binary systems with initial eccentric orbit ($e > 0.6$). Therefore, we expect that initial distributions that favour eccentric orbits, like the thermal distribution, boost the number of Gaia BH3-like systems. In contrast, circular orbits significantly suppress the formation of such systems unless high kicks models are used.

In some cases, initial circular binaries are justified by the effect of tides. The `sevn` simulations used in this work implement the tides following the formalism by Hurley et al. (2002) (see also Iorio et al. 2023) and show that for Gaia BH3-like systems tides are extremely inefficient. The tidal efficiency is at its maximum after the main sequence phase of the BH progenitor, when the star expands and develops a convective envelope. Assuming that the dominant tidal dissipation mechanism is due to convective motions in the envelope (Zahn 1977; Hurley et al. 2002), and considering the `mist` models at $Z = 4.1 \times 10^{-5}$ (Figure 1), we estimate a circularisation timescale due to tides of $\tau_{\text{circ}} \approx 10^{25} - 10^{38} \text{ Gyr}$. This timescale is orders of magnitude longer than the lifetime of the binary system and especially longer than the post-main-sequence phase, when tides are more efficient.

4.2. Systematic uncertainties

Table 1 shows that the formation efficiency of BH-star systems drops significantly for models with high supernova kicks. In the

models VK100 and VK265, we can exclude the hypothesis that the observation of Gaia BH3 is consistent with the isolated channel at a high level of significance ($> 3\sigma$). Estimates of BH kicks rely on a few tracers (e.g. X-ray binaries) and are subjected to many uncertainties and systematics (see e.g. Andrews & Kalogera 2022; Atri et al. 2019; Shenar et al. 2022a). The association of Gaia BH3 with a stellar stream (Balbinot et al. 2024) indicates that the binary system did not experience a kick much higher than the typical escape velocity from a star cluster ($< 10 \text{ km/s}$) at the time of BH formation.

In our analysis, we are not considering binaries with companion stars less massive than $0.71 M_{\odot}$. As discussed by El-Badry (2024), such a population can represent a significant portion of the stellar companions of Gaia BH3-like systems. To assess its relevance on the estimate of the formation efficiency, we generate new initial conditions as in Section 2.1, but assuming an extended mass ratio range from $0.08 M_{\odot}/m_1$ to 1. We find that the percentage of binaries hosting a BH progenitor and a secondary star less massive than $0.71 M_{\odot}$ is 40% of similar binaries with a secondary in the mass range $0.71 - 1.0 M_{\odot}$. Therefore, we expect an overall increase of the formation efficiency of about 40% with respect to the value reported in Table 1. This factor is balanced by the commonly assumed binary fraction in stellar populations (40 – 60%, see e.g. Moe & Di Stefano 2017).

Although the formation of Gaia BH3 does not depend on binary processes such as common envelope and mass transfer, the uncertainties in the stellar evolution models can have an important impact on this study. For instance, differences in the maximum radius of the BH progenitor are fundamental to select what objects interact during binary evolution. Different wind prescriptions are fundamental to set the final relation between the initial mass and the BH mass. El-Badry (2024) explored the main uncertainties about stellar evolution models showing that systems such as Gaia BH3 can be produced within a reasonable range of stellar parameters including initial mass, metallicity, stellar rotation, and convection models.

Many population synthesis studies on BH-star binaries are based on stellar evolution models by Pols et al. (1998) (see e.g. Breivik et al. 2017; Shao & Li 2019; Chawla et al. 2022; Shikauchi et al. 2023). In general, the stars in these tracks tend to expand to larger radii compared to the `mist` models. Most of these works focus on the Galactic population of which the stellar halo is a negligible component, hence a direct comparison is not straightforward. We notice that the properties of the few metal-poor stars reported by Chawla et al. (2022) seem to be qualitatively consistent with the distribution of BH-star systems in terms of period and BH mass.

4.3. Alternative formation channel

Gaia BH3 is associated with the ED-2 stream (Balbinot et al. 2024), therefore it possibly spent a part of its life in a dynamical environment. The variety of interactions in dynamical environments have two competitive effects. On the one hand, they can pair BHs and stars or create binary systems with orbital properties (e.g., high eccentricities) that boost the production of Gaia BH3-like binaries. On the other hand, dynamical interactions could destroy original and newly formed BH-star systems, especially if their orbit is wide and the companion star is low mass.

The other two BH-star systems retrieved from Gaia data (BH1 El-Badry et al. 2023b, and BH2 El-Badry et al. 2023a) are difficult to reconcile with isolated binary evolution models (El-Badry et al. 2023a), while they are more easily formed in

star clusters (Rastello et al. 2023; Di Carlo et al. 2024; Tanikawa et al. 2024; Kotko et al. 2024).

Marín Pina et al. (2024) show that BH-star systems dynamically form in an efficient way in globular clusters with mass $10^5 - 10^6 M_{\odot}$. They estimate a formation efficiency of $10^{-5} - 3 \times 10^{-4} M_{\odot}^{-1}$ by considering all the BH-star systems formed in their simulations (both escaped or retained in the cluster). Their proposed dynamical channel is one to two orders of magnitude times more efficient than the isolated channel presented in this work. However, when considering the halo (Deason et al. 2019) and the cluster radial profile (e.g., Gieles & Gnedin 2023), the difference on the expected formation efficiency of BH-star systems in the solar neighbourhood reduces to a factor of 3–10. If Gaia BH3 remains the only observed BH-star system in the halo, none of the two formation channels can be excluded or significantly favoured.

When focusing specifically on Gaia BH3-like systems, Marín Pina et al. (2024) find that only 0.6% of their BH-star systems fall within the same selection box used in our work (Figure 2). This fraction is a factor of 3–5 smaller than what we found in our isolated-binary simulations. Taken at face value, these numbers seem to indicate that the dynamic environment does not considerably boost the formation of Gaia BH3-like systems. Therefore, even if it was clearly born in a cluster, Gaia BH3 is compatible with a primordial binary star which escaped from the cluster without experiencing significant dynamical interactions.

We point out that our models can easily reproduce the physical properties of Gaia BH3 with low or negligible BH natal kicks. Thus, they also point towards an efficient retention of the so-formed binary within the star cluster where it was born. As a consequence, our isolated formation scenario can account for the formation of Gaia BH3 in a low-density and dynamically-quiet star cluster, while being consistent with its membership in a stellar stream like ED-2 (Balbinot et al. 2024).

A more quantitative comparison and model selection requires a detailed analysis of systematic, selection effects, channel definitions, halo population models, and robust statistic tool (see e.g. Mould et al. 2023) that are beyond the scope of this paper.

5. Summary

We have explored the formation of Gaia BH3 (Gaia Collaboration et al. 2024), a non interacting binary system composed of a massive BH ($\approx 30 M_{\odot}$) and a low-mass giant star ($\approx 0.8 M_{\odot}$), by means of population synthesis simulations.

We have exploited the flexibility of our code SEVN (Iorio et al. 2023) to perform the first population study of BH-star systems using the MIST stellar models (Choi et al. 2016). We explored the parameter space by considering 9 different metallicities, 4 different supernova kick models, 2 models for the common envelope efficiency parameter α , and 2 models for the onset of Roche-Lobe overflow. Also, we implemented a Bayesian sampling analysis to study the distribution of initial conditions that reproduce exactly the observed properties of Gaia BH3.

The main takeaways of our analysis are as follows.

- Systems like Gaia BH3 represent a common product of isolated binary evolution at low metallicity ($Z < 0.01$). They form preferentially from a massive star (40–60 M_{\odot}) in an initially wide ($P > 10^3$ days) and eccentric ($e > 0.6$) orbit with a low mass companion. The progenitor binary system never underwent Roche-lobe overflow during its life.

- Our fiducial supernova kick model (Giacobbo & Mapelli 2020) produces low natal kicks, leaving the initial orbital properties of the binary systems almost unchanged. The formation of Gaia BH3 is possible up to kicks as high as 220 km/s, but this requires fine tuning for the conditions at BH formation, and the overall formation efficiency drops by about one order of magnitude.
- Focusing on systems older than 10 Gyr, we find a formation efficiency $\eta_{\text{BHStar}} \sim 10^{-6} M_{\odot}^{-1}$ for BH-star binaries in general, and $\eta_{\text{GaiaBH3-like}} \sim 5 \times 10^{-8} M_{\odot}^{-1}$ for Gaia BH3-like systems.
- Considering the Galactic stellar halo model by Deason et al. (2019), we expect up to ≈ 3000 BH-star systems born in the stellar halo from isolated evolution. About 50–100 of them are Gaia BH3-like systems in terms of mass and orbital properties. Given these numbers, the hypothesis that Gaia BH3 formed through isolated evolution cannot be ruled out at 3 σ significance level.
- Comparing our formation efficiencies with the ones derived by Marín Pina et al. (2024) for the dynamical formation scenario, we conclude that none of the two channels is strongly favoured for the formation of Gaia BH3.

Overall, Gaia BH3 is compatible with a primordial, metal-poor binary system that never evolved via Roche-lobe overflow. If it formed in a star cluster, it might have evolved nearly unperturbed until it quietly evaporated from it or was dynamically ejected. Unlike Gaia BH1 and BH2, its orbital properties are easy to explain with current stellar and binary evolution models.

Acknowledgements. We thank Daniel Marín Pina for useful comments. Part of this work was supported by the German *Deutsche Forschungsgemeinschaft*, DFG project number Ts 17/2–1. MM, GI, ST, MD, StR, GE, EK, EL and MPV acknowledge financial support from the European Research Council for the ERC Consolidator grant DEMOBLACK, under contract no. 770017. MM, ST, StR and MPV also acknowledge financial support from the German Excellence Strategy via the Heidelberg Cluster of Excellence (EXC 2181 - 390900948) STRUCTURES. MD also acknowledges financial support from Cariparo foundation under grant 55440. AAT acknowledges support from the European Union’s Horizon 2020 and Horizon Europe research and innovation programs under the Marie Skłodowska-Curie grant agreements no. 847523 and 101103134. SaR acknowledges support from the Beatriu de Pinós postdoctoral program under the Ministry of Research and Universities of the Government of Catalonia (Grant Reference No. 2021 BP 00213). MAS acknowledges funding from the European Union’s Horizon 2020 research and innovation programme under the Marie Skłodowska-Curie grant agreement No. 101025436 (project GRACE-BH, PI: Manuel Arca Sedda). MAS acknowledge financial support from the MERAC Foundation.

References

- Abbott, B. P., Abbott, R., Abbott, T. D., et al. 2016a, *Phys. Rev. Lett.*, **116**, 061102 [arXiv:1602.03837]
- Abbott, B. P., Abbott, R., Abbott, T. D., et al. 2016b, *Phys. Rev. Lett.*, **116**, 241102 [arXiv:1602.03840]
- Abbott, R., Abbott, T. D., Abraham, S., et al. 2021a, *Physical Review X*, **11**, 021053 [arXiv:2010.14527]
- Abbott, R., Abbott, T. D., Acernese, F., et al. 2021b, *arXiv e-prints*, arXiv:2111.03606 [arXiv:2111.03606]
- Abbott, R., Abbott, T. D., Acernese, F., et al. 2021c, *arXiv e-prints*, arXiv:2108.01045 [arXiv:2108.01045]
- Andrews, J. J. & Kalogera, V. 2022, *ApJ*, **930**, 159 [arXiv:2203.15156]
- Atri, P., Miller-Jones, J. C. A., Bahramian, A., et al. 2019, *MNRAS*, **489**, 3116 [arXiv:1908.07199]
- Balbinot, E., Dodd, E., Matsuno, T., et al. 2024, *arXiv e-prints*, arXiv:2404.11604 [arXiv:2404.11604]
- Belczynski, K., Bulik, T., Fryer, C. L., et al. 2010, *ApJ*, **714**, 1217 [arXiv:0904.2784]

- Belczynski, K., Heger, A., Gladysz, W., et al. 2016, *A&A*, **594**, A97 [arXiv:1607.03116]
- Bell, E. F., Zucker, D. B., Belokurov, V., et al. 2008, *ApJ*, **680**, 295 [arXiv:0706.0004]
- Breivik, K., Chatterjee, S., & Larson, S. L. 2017, *ApJ*, **850**, L13 [arXiv:1710.04657]
- Casares, J., Negueruela, I., Ribó, M., et al. 2014, *Nature*, **505**, 378 [arXiv:1401.3711]
- Chawla, C., Chatterjee, S., Breivik, K., et al. 2022, *ApJ*, **931**, 107 [arXiv:2110.05979]
- Choi, J., Dotter, A., Conroy, C., et al. 2016, *ApJ*, **823**, 102 [arXiv:1604.08592]
- Claeys, J. S. W., Pols, O. R., Izzard, R. G., Vink, J., & Verbunt, F. W. M. 2014, *A&A*, **563**, A83 [arXiv:1401.2895]
- Costa, G., Bressan, A., Mapelli, M., et al. 2021, *MNRAS*, **501**, 4514 [arXiv:2010.02242]
- Costa, G., Mapelli, M., Iorio, G., et al. 2023, *arXiv e-prints*, arXiv:2303.15511 [arXiv:2303.15511]
- Deason, A. J., Belokurov, V., & Sanders, J. L. 2019, *MNRAS*, **490**, 3426 [arXiv:1908.02763]
- Di Carlo, U. N., Agrawal, P., Rodriguez, C. L., & Breivik, K. 2024, *ApJ*, **965**, 22 [arXiv:2306.13121]
- Eggleton, P. P. 1983, *ApJ*, **268**, 368
- El-Badry, K. 2024, *arXiv e-prints*, arXiv:2404.13047 [arXiv:2404.13047]
- El-Badry, K., Rix, H.-W., Cendes, Y., et al. 2023a, *MNRAS*, **521**, 4323
- El-Badry, K., Rix, H.-W., Quataert, E., et al. 2023b, *MNRAS*, **518**, 1057 [arXiv:2209.06833]
- Farmer, R., Renzo, M., de Mink, S. E., Marchant, P., & Justham, S. 2019, *ApJ*, **887**, 53 [arXiv:1910.12874]
- Foreman-Mackey, D., Hogg, D. W., Lang, D., & Goodman, J. 2013, *PASP*, **125**, 306 [arXiv:1202.3665]
- Fryer, C. L., Belczynski, K., Wiktorowicz, G., et al. 2012, *ApJ*, **749**, 91 [arXiv:1110.1726]
- Gaia Collaboration, Panuzzo, P., Mazeh, T., et al. 2024, *arXiv e-prints*, arXiv:2404.10486 [arXiv:2404.10486]
- Gaia Collaboration, Vallenari, A., Brown, A. G. A., et al. 2023, *A&A*, **674**, A1 [arXiv:2208.00211]
- Generozov, A. & Perets, H. B. 2024, *ApJ*, **964**, 83 [arXiv:2312.03066]
- Giacobbo, N. & Mapelli, M. 2020, *ApJ*, **891**, 141 [arXiv:1909.06385]
- Gieles, M. & Gnedin, O. Y. 2023, *MNRAS*, **522**, 5340 [arXiv:2303.03791]
- Giesers, B., Dreizler, S., Husser, T.-O., et al. 2018, *MNRAS*, **475**, L15 [arXiv:1801.05642]
- Giesers, B., Kamann, S., Dreizler, S., et al. 2019, *A&A*, **632**, A3 [arXiv:1909.04050]
- Guseinov, O. K. & Zel'dovich, Y. B. 1966 *Soviet Ast.*, **10**, 251
- Heger, A. & Woosley, S. E. 2002, *ApJ*, **567**, 532 [arXiv:astro-ph/0107037]
- Hobbs, G., Lorimer, D. R., Lyne, A. G., & Kramer, M. 2005, *MNRAS*, **360**, 974 [arXiv:astro-ph/0504584]
- Hurley, J. R., Tout, C. A., & Pols, O. R. 2002, *MNRAS*, **329**, 897 [arXiv:astro-ph/0201220]
- Hut, P. 1981 *A&A*, **99**, 126
- Iorio, G., Belokurov, V., Erkal, D., et al. 2018, *MNRAS*, **474**, 2142 [arXiv:1707.03833]
- Iorio, G., Mapelli, M., Costa, G., et al. 2023, *MNRAS*, **524**, 426 [arXiv:2211.11774]
- Ivanova, N., Justham, S., Chen, X., et al. 2013, *A&A Rev.*, **21**, 59 [arXiv:1209.4302]
- Kotko, I., Banerjee, S., & Belczynski, K. 2024, *arXiv e-prints*, arXiv:2403.13579 [arXiv:2403.13579]
- Kroupa, P. 2001, *MNRAS*, **322**, 231 [arXiv:astro-ph/0009005]
- Lane, J. M. M., Bovy, J., & Mackereth, J. T. 2023, *MNRAS*, **526**, 1209 [arXiv:2306.03084]
- Lennon, D. J., Dufton, P. L., Villaseñor, J. I., et al. 2022, *A&A*, **665**, A180 [arXiv:2111.12173]
- Mahy, L., Sana, H., Shenar, T., et al. 2022, *A&A*, **664**, A159 [arXiv:2207.07752]
- Mapelli, M., Colpi, M., & Zampieri, L. 2009, *MNRAS*, **395**, L71 [arXiv:0902.3540]
- Mapelli, M., Ripamonti, E., Zampieri, L., Colpi, M., & Bressan, A. 2010, *MNRAS*, **408**, 234 [arXiv:1005.3548]
- Mapelli, M., Spera, M., Montanari, E., et al. 2020, *ApJ*, **888**, 76 [arXiv:1909.01371]
- Mapelli, M., Zampieri, L., Ripamonti, E., & Bressan, A. 2013, *MNRAS*, **429**, 2298 [arXiv:1211.6441]
- Marín Pina, D., Rastello, S., Gieles, M., et al. 2024 *arXiv e-prints*, arXiv:2404.13036 [arXiv:2404.13036]
- Medina, G. E., Muñoz, R. R., Carlin, J. L., et al. 2024, *arXiv e-prints*, arXiv:2402.14055 [arXiv:2402.14055]
- Miller-Jones, J. C. A., Bahramian, A., Orosz, J. A., et al. 2021, *Science*, **371**, 1046 [arXiv:2102.09091]
- Moe, M. & Di Stefano, R. 2017, *ApJS*, **230**, 15 [arXiv:1606.05347]
- Mould, M., Gerosa, D., Dall'Amico, M., & Mapelli, M. 2023, *MNRAS*, **525**, 3986 [arXiv:2305.18539]
- Oëzel, F., Psaltis, D., Narayan, R., & McClintock, J. E. 2010, *ApJ*, **725**, 1918 [arXiv:1006.2834]
- Penoyre, Z., Belokurov, V., & Evans, N. W. 2022, *MNRAS*, **513**, 2437 [arXiv:2111.10380]
- Pols, O. R., Schröder, K.-P., Hurley, J. R., Tout, C. A., & Eggleton, P. P. 1998, *MNRAS*, **298**, 525
- Rastello, S., Iorio, G., Mapelli, M., et al. 2023, *MNRAS*, **526**, 740 [arXiv:2306.14679]
- Ribó, M., Munar-Adrover, P., Paredes, J. M., et al. 2017, *ApJ*, **835**, L33 [arXiv:1701.07265]
- Sana, H., de Mink, S. E., de Koter, A., et al. 2012, *Science*, **337**, 444 [arXiv:1207.6397]
- Saracino, S., Kamann, S., Guarcello, M. G., et al. 2022, *MNRAS*, **511**, 2914 [arXiv:2111.06506]
- Saracino, S., Shenar, T., Kamann, S., et al. 2023, *MNRAS*, **521**, 3162 [arXiv:2303.07369]
- Sgalletta, C., Iorio, G., Mapelli, M., et al. 2023, *arXiv e-prints*, arXiv:2305.04955 [arXiv:2305.04955]
- Shao, Y. & Li, X.-D. 2019, *ApJ*, **885**, 151 [arXiv:1909.11328]
- Shenar, T., Sana, H., Mahy, L., et al. 2022a, *Nature Astronomy*, **6**, 1085 [arXiv:2207.07675]
- Shenar, T., Sana, H., Mahy, L., et al. 2022b, *A&A*, **665**, A148 [arXiv:2207.07674]
- Shikauchi, M., Tsuna, D., Tanikawa, A., & Kawanaka, N. 2023, *ApJ*, **953**, 52 [arXiv:2301.07207]
- Spera, M. & Mapelli, M. 2017, *MNRAS*, **470**, 4739 [arXiv:1706.06109]
- Spera, M., Mapelli, M., & Bressan, A. 2015, *MNRAS*, **451**, 4086 [arXiv:1505.05201]
- Spera, M., Mapelli, M., Giacobbo, N., et al. 2019, *MNRAS*, **485**, 889 [arXiv:1809.04605]
- Tanikawa, A., Cary, S., Shikauchi, M., Wang, L., & Fujii, M. S. 2024, *MNRAS*, **527**, 4031 [arXiv:2303.05743]
- Tanikawa, A., Hattori, K., Kawanaka, N., et al. 2023, *ApJ*, **946**, 79 [arXiv:2209.05632]
- Tanikawa, A., Susa, H., Yoshida, T., Trani, A. A., & Kinugawa, T. 2021, *ApJ*, **910**, 30 [arXiv:2008.01890]
- Thompson, T. A., Kochanek, C. S., Stanek, K. Z., et al. 2019, *Science*, **366**, 637 [arXiv:1806.02751]
- Trimble, V. L. & Thorne, K. S. 1969, *ApJ*, **156**, 1013

- Webbink, R. F. 1984, *ApJ*, 277, 355
- Woosley, S. E. 2017, *ApJ*, 836, 244 [arXiv:1608.08939]
- Woosley, S. E. 2019, *ApJ*, 878, 49 [arXiv:1901.00215]
- Zahn, J. P. 1977A&A, 57, 383
- Zampieri, L. & Roberts, T. P. 2009, *MNRAS*, 400, 677
[arXiv:0909.1017]
- Ziosi, B. M., Mapelli, M., Branchesi, M., & Tormen, G. 2014,
MNRAS, 441, 3703 [arXiv:1404.7147]